

Leakage channel fibers with microstructured cladding elements: A unique LMA platform

Sonali Dasgupta,^{1,2*} John R Hayes,¹ and David J Richardson¹

¹Optoelectronic Research Centre, University of Southampton, Southampton SO17 1BJ, UK

²LightCUE, Bangalore 560076, India

*sxd@orc.soton.ac.uk

Abstract: We present a novel design of leakage channel fiber (LCF) that incorporates an air-hole lattice to define the modal filtering characteristics. The approach has the potential to offer single-mode, large mode area (LMA) fibers in a single-material platform with bend loss characteristics comparable to all-solid (LCFs) whilst at the same time providing significant fabrication benefits. We compare the performance of the proposed fiber with that of rod-type photonic crystal fibers (PCFs) and all-solid LCFs offering a similar effective mode area of $\sim 1600\mu\text{m}^2$ at $1.05\mu\text{m}$. Our calculations show that the proposed fiber concept succeeds in combining the advantages of the use of small air holes and the larger design space of rod-type PCFs with the improved bend tolerance and greater higher order mode discrimination of all-solid LCFs, while alleviating their respective issues of rigidity and restricted material design space. We report the fabrication and experimental characterization of a first exemplar fiber, which we demonstrate offers a single-mode output with a fundamental mode area $\sim 1440\mu\text{m}^2$ at $1.06\mu\text{m}$, and that can be bent down to a radius of 20cm with a bend loss of $< 3\text{dB/turn}$. Finally we show that the proposed design concept can be adopted to achieve larger mode areas ($> 3000\mu\text{m}^2$), albeit at the expense of reduced bend tolerance.

©2014 Optical Society of America

OCIS codes: (060.4005) Microstructured fibers; (060.5295) Photonic crystal fibers; (060.2280) Fiber design and fabrication; (060.2400) Fiber properties; (060.2430) Fibers, single-mode.

References and links

1. Y. Jeong, A. J. Boyland, J. K. Sahu, S. Chung, J. Nilsson, and D. N. Payne, "Multi-kilowatt single-mode ytterbium-doped large-core fiber laser," *J. Opt. Soc. Korea* **13**(4), 416–422 (2009).
2. A. Malinowski, A. Piper, J. H. V. Price, K. Furusawa, Y. Jeong, J. Nilsson, and D. J. Richardson, "Ultrashort-pulse Yb³⁺-fiber-based laser and amplifier system producing $>25\text{-W}$ average power," *Opt. Lett.* **29**(17), 2073–2075 (2004).
3. F. Röser, T. Eidam, J. Rothhardt, O. Schmidt, D. N. Schimpf, J. Limpert, and A. Tünnermann, "Millijoule pulse energy high repetition rate femtosecond fiber chirped-pulse amplification system," *Opt. Lett.* **32**(24), 3495–3497 (2007).
4. <http://phys.org/news/2013-06-incoherent-combining-fiber-lasers-energy.html>
5. P. F. Moulton, "High power Tm:silica fiber lasers: Current status, prospects and challenges," in *CLEO/Europe and EQEC 2011 Conference Digest* (Optical Society of America, 2011), paper TF2_3.
6. M. Petrovich, N. Baddela, N. Wheeler, E. Numkam, R. Slavik, D. Gray, J. Hayes, J. Wooler, F. Poletti, and D. Richardson, "Development of low loss, wide bandwidth hollow core photonic bandgap fibers," in *Optical Fiber Communication Conference/National Fiber Optic Engineers Conference* (Optical Society of America, 2013), paper OTh1J.3.
7. S. D. Jackson, "Towards high-power mid-infrared emission from a fibre laser," *Nat. Photonics* **6**(7), 423–431 (2012).
8. D. J. Richardson, J. Nilsson, and W. A. Clarkson, "High power fiber lasers: Current status and future perspectives," *J. Opt. Soc. Am. B* **27**(11), B63 (2010).
9. T. Hault, J. Gabzdyl, and K. Dzurko, "Fiber lasers in solar applications," in *Solar Energy: New Materials and Nanostructured Devices for High Efficiency* (Optical Society of America, 2008), paper STuC3.
10. P. Kah, J. Lu, J. Martikainen, and R. Suoranta, "Remote laser welding with high power fiber lasers," *Engineering* **05**(09), 700–706 (2013).

11. H. Meng, J. Liao, Y. Zhou, and Q. Zhang, "Laser micro-processing of cardiovascular stent with fiber laser cutting system," *Opt. Laser Technol.* **41**(3), 300–302 (2009).
12. W. W. Ke, X. J. Wang, X. F. Bao, and X. J. Shu, "Thermally induced mode distortion and its limit to power scaling of fiber lasers," *Opt. Express* **21**(12), 14272–14281 (2013).
13. J. Limpert, N. Deguil-Robin, I. Manek-Hönninger, F. Salin, F. Röser, A. Liem, T. Schreiber, S. Nolte, H. Zellmer, A. Tünnermann, J. Broeng, A. Petersson, and C. Jakobsen, "High-power rod-type photonic crystal fiber laser," *Opt. Express* **13**(4), 1055–1058 (2005).
14. J. Limpert, O. Schmidt, J. Rothhardt, F. Röser, T. Schreiber, A. Tünnermann, S. Ermeneux, P. Yvernault, and F. Salin, "Extended single-mode photonic crystal fiber lasers," *Opt. Express* **14**(7), 2715–2720 (2006).
15. F. Jansen, F. Stutzki, T. Eidam, J. Rothhardt, S. Hädrich, H. Carstens, C. Jauregui, J. Limpert, and A. Tünnermann, "Yb-doped Large Pitch Fiber with 105 μ m Mode Field Diameter," in *Optical Fiber Communication Conference/National Fiber Optic Engineers Conference*, (Optical Society of America, 2011), paper OTuC.
16. T. A. Birks, J. C. Knight, and P. S. Russell, "Endlessly single-mode photonic crystal fiber," *Opt. Lett.* **22**(13), 961–963 (1997).
17. L. Dong, X. Peng, and J. Li, "Leakage channel optical fibers with large effective area," *J. Opt. Soc. Am. B* **24**(8), 1689 (2007).
18. L. Dong, T. Wu, H. A. McKay, L. Fu, J. Li, and H. G. Winful, "All-glass large-core leakage channel fibers," *IEEE J. Sel. Top. Quantum Electron.* **15**(1), 47–53 (2009).
19. E. M. Dianov, K. M. Golant, V. I. Karpov, R. R. Khrapko, A. S. Kurkov, V. M. Mashinsky, and V. N. Protopopov, "Fluorine-doped silica optical fibres fabricated using plasma chemical technologies," *Proc. SPIE* **2425**, 53–57 (1994).
20. S. Dasgupta, J. R. Hayes, C. Baskiotis, and D. J. Richardson, "Novel all-silica large mode area fiber with microstructured cladding element," in *SPIE Photonics West, LASE* (San Francisco, 2013).
21. T. W. Wu, L. Dong, and H. Winful, "Bend performance of leakage channel fibers," *Opt. Express* **16**(6), 4278–4285 (2008).
22. D. Marcuse, "Influence of curvature on the losses of doubly clad fibers," *Appl. Opt.* **21**(23), 4208–4213 (1982).

1. Introduction

The industrial need for cost-effective and compact high power laser sources has driven the rapid development and commercialization of fiber laser technology, leading to the host of innovative products to be found in the market place today. Continuous wave fiber laser systems operating with multi-kW average powers and short pulse systems operating at peak powers of up to ~ 1 GW are now considered indispensable tools in a host of important application areas that include: industrial materials processing (e.g. for welding, cutting and marking), defense (e.g. for directed energy application and countermeasures), fundamental science (e.g. for generating laser-induced plasmas and particle acceleration), and medicine (e.g. for various imaging modalities and surgical procedures) [1–11].

Central to the power scaling of fiber lasers has been the development of large mode area (LMA) fibers capable of supporting and sustaining the ever increasing power levels. Rare earth doped LMA fibers are essential to the development of the lasers themselves and passive variants are important in fiber-based delivery of the beam directly from the laser output to where the laser light is ultimately to be used (which is often over a distance much longer than the length of fiber used in the laser itself). While hollow core bandgap fibers have recently garnered a lot of attention for high power beam delivery applications [6], here we seek a fiber design that is applicable to fiber lasers and amplifiers, which require a rare-earth doped silica glass core. Besides supporting a large fundamental mode (FM) area, state-of-the-art LMA fibers also need to be able to provide a number of critically important practical features. These include robust single-mode output, low fundamental mode loss and low bend loss sensitivity. Indeed, in the majority of commercially relevant cases a compromise needs to be struck between the use of fibers offering the maximum possible effective area and those offering better performance with regards to these more practical issues. Such considerations are beginning to significantly constrain system performance – particularly in the pulsed fiber laser area where nonlinear effects associated with high peak powers are the dominant consideration. Consequently, new approaches to LMA fibers offering different opportunities for trade-off between the key properties listed above are critical to the further development (and deployment) of fiber laser technology. For completeness, we note that the active management of beam distortion due to thermal load and optical nonlinearity through fiber

design are also emerging topics [12]. However, these issues are beyond the scope of the current paper.

Rod-type Photonic Crystal Fibers (PCFs) have been very successful in offering large mode areas [13,14], however such fibers are extremely bend loss sensitive and the need to keep them rigid and straight means the typical device length is limited to ~ 1 m, which restricts their application in many real-life systems. Similar limitations govern the more recently reported large pitch fibers that can to a large extent be considered a subset of rod-type PCFs, although they have been shown to exhibit very large mode areas up to $\sim 8600 \mu\text{m}^2$ [15]. Thus, LMA fibers offering a certain degree of bend tolerance are highly desirable, and leakage channel fibers (LCFs) have attracted a lot of attention in this regard. Unlike the rod-type PCFs that are based on the endlessly single-mode feature of PCFs [16], LCFs exploit the large differential leakage loss of the modes in a leaky fiber structure to achieve single mode output along with low bend loss for considerably large mode areas [17]. The initial reports of LCFs showed their potential to offer mode areas of $\sim 1500 \mu\text{m}^2$ with a critical bend radius of 20 cm [17]. However, in spite of such remarkable performance, the use of large air holes (hole diameter $> 30 \mu\text{m}$) to define the leakage channels and their inevitable collapse/distortion during splicing/end termination renders air-hole LCFs impractical. A solution was proposed in the form of all-solid LCFs in which the air holes were replaced by F-doped rods [18]. These LCFs offer optical mode characteristics at par with the air-hole LCFs and their properties can be tailored by controlling the index difference between the core and the cladding rods. For example, a larger index difference enables a higher effective index difference between the modes, a lower mode loss sensitivity to index variations and reduced losses at smaller hole diameter to pitch ratio. However, in practice, the material design space is quite limited in the all-solid LCFs. In our experience, one of the most challenging issues when incorporating elements drawn from brought-in F-doped silica is that of bubble formation during fiber draw [19]. We note that the low draw speeds typical of special fiber fabrication and the large combined surface area of the elements inside a stacked preform, provide potential for bubble formation, which results in issues of poor surface quality and localized defects that can severely compromise fiber quality. This may be especially important where a large index contrast is created using a glass in which the dopant is not in thermodynamic equilibrium as is the case for high concentrations of fluorine [19]. These considerations can limit the maximum material index difference that is practical in F-doped rods to $\sim 10^{-3}$ although F-doped preforms with an index difference of $\sim 2.3 \times 10^{-2}$ are commercially available. In fact, to the best of our knowledge, the maximum material index difference reported in fabricated all-solid LCFs to date has been limited to 1.2×10^{-3} . In contrast, the proposed design, referred to as the micro-clad LCF from hereon, obviates the aforementioned issues by exploiting the higher index contrast of silica/air and the simplicity of a single material structure.

The micro-clad LCFs are based on the ‘leakage channel’ concept but alleviate the design limitations of the conventional LCFs and rod-type fibers while offering the advantages of these two very successful concepts in their own right, through a single fiber design [20]. We present fabrication and characterization results of a first exemplar micro-clad LCF and compare its performance with equivalent all-solid LCFs and rod-type PCFs.

2. Fiber design concept and simulation results

The micro-clad LCF (c.f. Figure 1(c)) consists of 6 microstructured cladding elements that are arranged in a hexagonal lattice and surround the core region (pitch, Λ_1). Each cladding element itself is a hexagonal lattice of ~ 3 -4 rings (n_{rings}) of small air holes (hole diameter, d_2 ($\sim 1 \mu\text{m}$), pitch, Λ_2). The separation between these microstructured cladding elements defines the “leakage channels” that enable higher order mode (HOM) filtering by allowing them to preferentially leak out from these silica “channels” while substantially confining the FM within the core region (large differential modal loss). In contrast to previously reported

designs of LCFs that employed large air holes or F-doped rods, the position and lattice design of the microstructured elements in the micro-clad LCF determines the “effective index difference” between the core and the cladding, and its filtering capability. Both these properties in micro-clad LCFs can be precisely controlled by engineering the lattice of air holes (pitch and size of the air holes) in the microstructured cladding elements, thereby

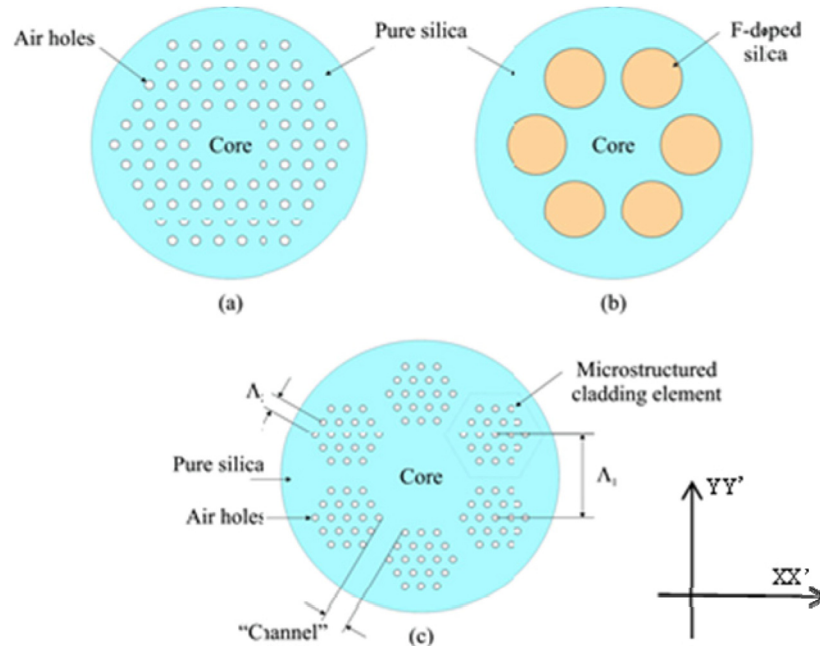


Fig. 1. Schematic of the cross-sectional view of (a) Rod-type PCF (b) All-solid LCF (c) proposed micro-clad LCF.

offering a much greater control and tunability over the achievable “numerical aperture” as compared to conventional LCF approaches. It has been reported in [18] that a larger index difference between the core and the cladding region increases the differential loss and modal index difference between the FM and HOMs, both of which are crucial in high power applications. Precise control over the air-hole lattice structure offers a greater tunability and control over the index difference between the active core and silica cladding regions in fiber amplifiers / lasers. Thus, besides allowing easier fabrication of longitudinally consistent structures, the design also provides greater control and freedom to tailor the fiber properties. Simultaneously, the use of a single material and small air holes makes fabrication and integration to conventional optical fiber systems relatively straightforward and comparable to rod-type fibers that have already been commercialized and standardized to a certain extent.

2.1 Modal characteristics

The differential loss between the FM and the HOMs of the micro-clad LCF is predominantly determined by the separation between the cladding elements. We define the separation by σ ($= \Lambda_1 - n_{rings} \times \Lambda_2$) and which is related to the width of these channels. For the initial design, we arbitrarily choose a core diameter of $50\mu\text{m}$, and an air-hole diameter of $1\mu\text{m}$ in the cladding. We vary the pitch of the lattice structure (Λ_2) in the cladding elements, which translates into different values of the channel width, σ , and study its effect on the modal characteristics of the fiber. Figure 2 illustrates the dependence of the FM effective area, FM loss and differential loss ratio (ratio between the propagation loss of the FM and the LP_{11} mode) on σ , which in turn relates to the pitch, number of rings and diameter of the small air

holes. We fitted the curves in Fig. 2 to obtain the empirical dependence of the fiber properties on σ . While the loss ratio and FM effective area follow a second order polynomial dependence on σ , the FM loss increases exponentially with an increase in σ . If we assume that the maximum FM loss that can be tolerated in a practical system is 1dB/m, a not unreasonable figure in many instances, Fig. 2(a) clearly shows that a FM effective area of up to $1900\mu\text{m}^2$ can be achieved with a core diameter of $50\mu\text{m}$ while maintaining a (linear) loss ratio between the FM and the first HOM (LP₁₁) > 22 (~13dB). It is also evident that there exists a trade-off between the largest effective area that can be attained, the lowest FM loss and the highest differential loss. Since

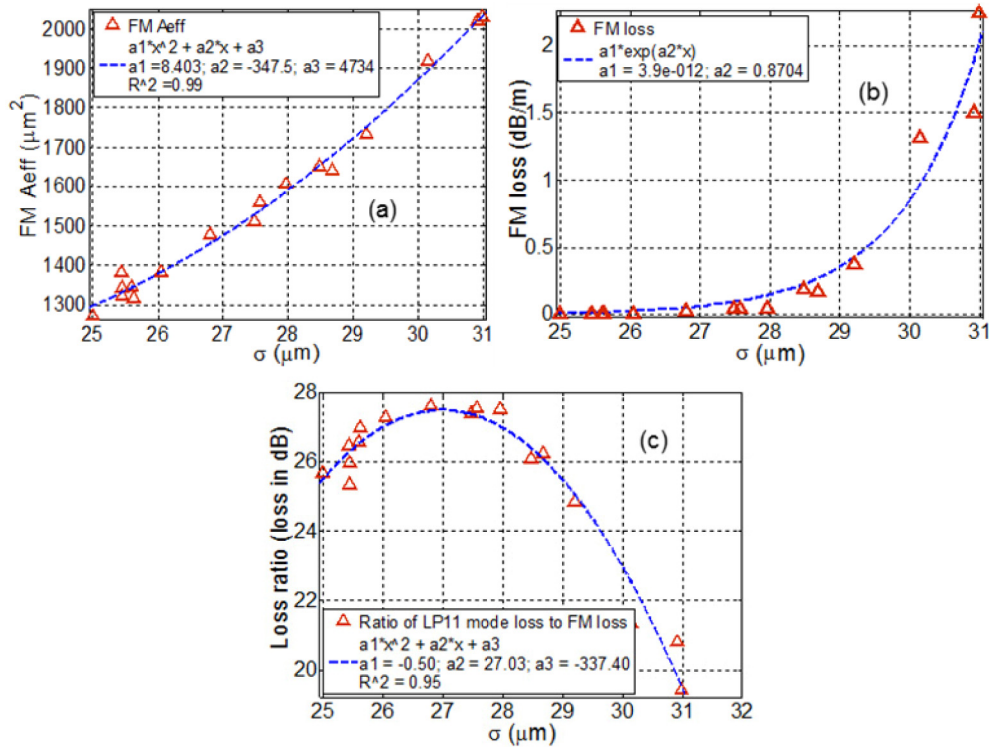


Fig. 2. Effect of cladding element separation, σ on (a) FM effective area (b) FM loss (c) Ratio of HOM loss to FM loss.

the FM loss has a much stronger exponential dependence on the channel separation than the differential loss, it ends up being the deciding factor for a particular design choice. It is interesting to note that around the peak of the loss ratio curve (Fig. 2(a)), the ratio itself is relatively insensitive to changes in the value of σ . This allows a much desired degree of design tolerance during fabrication. It is important to mention at this point that we observed the similar empirical dependence of FM effective area, FM loss and loss ratio for micro-clad LCFs with much larger effective areas (c.f. Sec.4.1).

2.2 Bend performance

Based on Fig. 2, we choose a LMA design that offers an effective area of $\sim 1600\mu\text{m}^2$ at $1.05\mu\text{m}$, with a FM and HOM loss of $\sim 0.05\text{dB/m}$ and 1dB/m , respectively. We confirmed that there are no other HOMs with lower losses that could compromise the single-modedness of the fiber. Figure 3 shows the power distribution of the LP₀₁ and LP₁₁ mode of the chosen fiber. We then study the bend performance of the design to analyze its feasibility for compact systems and in applications that require meter lengths of fiber (e.g. parabolic pulse amplifiers,

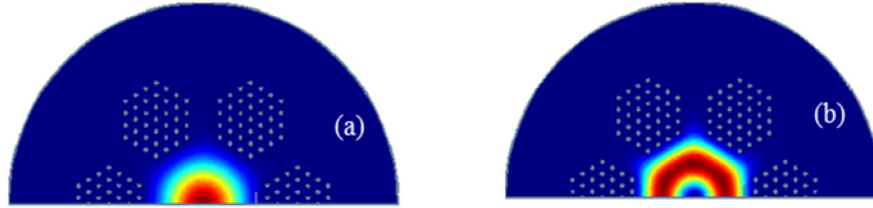


Fig. 3. Optical mode profile of the (a) LP_{01} and (b) LP_{11} modes of the designed fiber at $1.05\mu\text{m}$. We simulate only one half of the fiber to optimize computational time.

delivery fibers). Bending the fiber in almost all LMA designs not only increases the loss of the M, it also reduces the FM effective area, and in extremely small bends, distorts the mode shape. Figure 4 illustrates the change in effective area and loss of the FM of the designed fiber in the bent configuration (Rc is the bend radius); assuming the bend to be along the XX' plane (cf. Figure 1). Bending the fiber along the orthogonal YY' plane yields losses that are in line with the qualitative observations for all-solid LCFs [21]. Bend loss of the fiber is calculated using the equivalent index model defined in [22], which is implemented using the finite element solver COMSOL Multiphysics $\text{\textcircled{R}}$. Figure 4 shows that the fiber can be bent down to a radius of $\sim 45\text{cm}$ while maintaining the FM loss below 1dB/m .

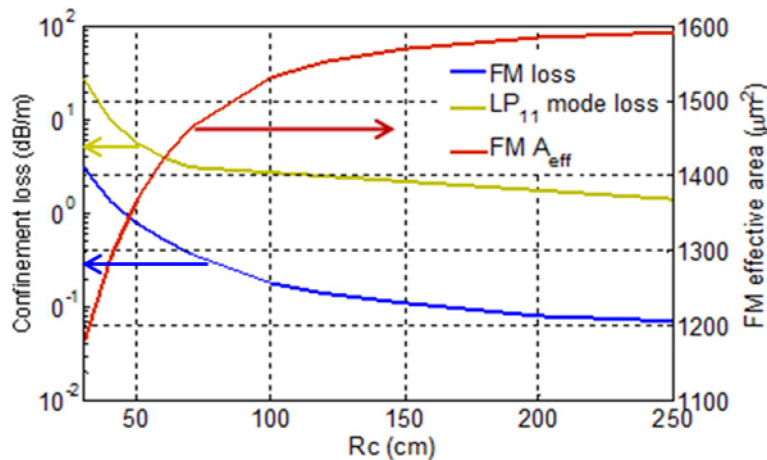


Fig. 4. Change in FM effective area, FM loss and LP_{11} mode loss with varying bend radii. Fiber core radius = $25\mu\text{m}$. $\Lambda_2 = 0.18$; air hole diameter = $1\mu\text{m}$.

This results in $\sim 20\%$ reduction in the effective area with $\sim 75\%$ confinement of the optical power within the notional core region. Tighter bends lead to a more significant reduction in the effective area and in addition to much higher FM propagation losses. Interestingly, bending the fiber does not seem to have a significant effect on the differential loss ratio although an optimum bending radius does exist that offers the largest ratio of loss between the FM and the first HOM. For even smaller bend radii, the loss ratio converges to a specific value (~ 7.2 in this case), depending on the fiber design.

2.3 Comparison with an equivalent all-solid LCF and rod-type PCF

In this section, we compare the performance of the designed micro-clad LCF with equivalent F-doped LCFs and a rod-type PCFs wherein equivalence implies that the fibers exhibit an equal effective FM area of $\sim 1600\mu\text{m}^2$ at $1.05\mu\text{m}$ in a straight configuration. Table 1 presents the results of the numerical comparison, wherein the designed micro-clad LCF is compared with two designs of all-solid LCF (based on F-doped rods) with different d/Λ , and two

designs of a typical rod-type PCF with 3 and 4 rings of air-holes, respectively. The first important observation is that the performance of the F-doped LCF and micro-clad LCFs are comparable,

Table 1. Comparison of various equivalent LMA designs at wavelength of 1.06 μ m

Fiber type	$d/\Lambda^{\#}$	$\Lambda^{\#}$ (μ m)	No. of rings of air holes	A_{eff} (μ m ²)	FM loss (dB/m)	LP ₁₁ loss (dB/m)	Loss ratio
Straight fiber properties							
Micro-clad LCF [#]	0.18	5.5	3	1605	0.04	1.2	27
All-solid LCF 1 [*]	0.78	45.1	1	1600	0.03	1.0	26
All-solid LCF 2 [*]	0.90	51.4	1	1608	1.5e-5	4.0e-4	26
Rod-type PCF 1 ^{**}	0.18	11.6	4	1596	7.4e-5	1.4e-3	18
Rod-type PCF 2 ^{**}	0.18	11.6	3	1596	4.7e-3	5.5e-2	11
Bent fiber properties, $R_c = 40$ cm							
Micro-clad LCF	0.18	5.5	3	1291	1.4	10.4	7.4
All-solid LCF 1 [*]	0.78	45.1	1	1293	1.1	7.9	7.0
All-solid LCF 2 [*]	0.90	51.4	1	1280	6.9e-4	4.2e-3	6.0
Rod-type PCF 1 ^{**}	0.18	11.6	4	1277	3.1e-3	1.3e-2	4.5
Rod-type PCF 2 ^{**}	0.18	11.6	3	1277	5.9e-2	0.2	3.4

* The index difference between the F-doped rods and pure silica is assumed to be 1.2×10^{-3}

** The PCFs are assumed to have a 19-cell core.

[#] Λ and d/Λ values correspond to d_2/Λ_2 and Λ_2 respectively, in case of the micro-clad LCF.

both in the straight and bent fiber configurations, which implies that the micro-clad LCFs offer an excellent alternative single-material platform to achieve the desirable optical characteristics of all-solid LCFs whilst providing an additional degree of design freedom to tune the index difference between the core and cladding (through the microstructured elements). The next significant observation is that although the rod-type PCFs offer large mode areas in a straight configuration, the loss ratio obtained in these fibers is much lower than that of the micro-clad LCFs. For example, if we extrapolate the results of the rod-type PCFs in Table 1 to infer the design parameters of the rod-type fiber that exhibits LP₁₁ loss > 1dB/m (so that the HOM loss is large enough to make the fiber device length practical), it can be deduced that we would either need to reduce the number of rings or the parameter, d/Λ , both of which would further reduce the differential loss. This in turn would make modal discrimination challenging other than in a strictly straight configuration. This has a crucial implication when we design fibers with larger effective areas (> 3000 μ m²): although we would need to resort to the straight configuration even for the micro-clad LCFs, they would offer a much better differential modal loss ratio than the rod-type PCFs, thus aiding in single-mode operation and providing more relaxed beam launch tolerances.

2.4 Rare earth doping

As previously mentioned this fiber type is intended for both beam delivery, in which case the core is undoped, and for high power generation, which requires incorporation of rare earth dopants in the core. The performance of micro-clad LCFs with an active core will depend significantly on the index difference between the doped (core) and undoped silica background

cladding) regions. In an ideal scenario, the doped core is index-matched with the pure silica so that the modal properties of the passive and active fiber are identical. However, in reality, rare-earth doping introduces a finite index difference and, we expect, an associated manufacturing tolerance. We therefore performed numerical simulations to study the sensitivity of the micro-clad LCFs to both positive and negative index differences between the core and the cladding glasses in order to identify acceptable bounds on this difference. Figure 5 shows that the micro-clad LCF is indeed reasonably sensitive to this difference and that an index difference of $\sim 10^{-4}$ between the doped core and the leakage channel regions is necessary to limit the change in effective area to within $\sim 10\%$ and the FM loss below $\sim 0.5\text{dB/m}$.

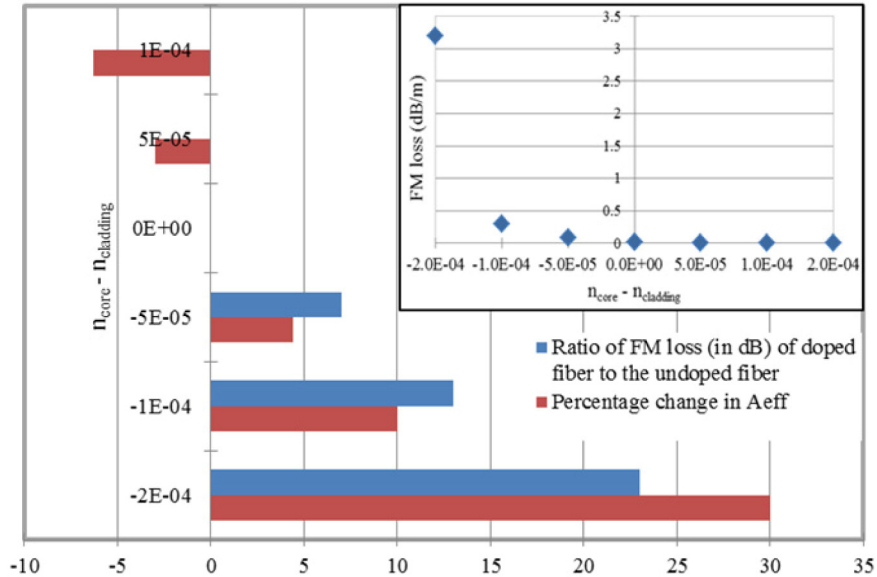


Fig. 5. Bar graph showing the effect of index difference between core and cladding (in an active micro-clad LCF) on the effective area and the FM loss. n_{core} and n_{cladding} are the refractive index of core and cladding, respectively. The inset shows the simulated FM loss values for the various values of index difference between core and cladding.

Further depression of the core index increases the FM loss further and affects the bend sensitivity of the design. It is worthwhile to mention that although we simulated the scenario of a positive index difference (core index $>$ silica glass) as well, which decreases the effective area, such a design would not be useful as the modes of the corresponding fiber would only support guided modes and would not offer any differential propagation loss/ mode filtering.

3. Fabrication and experimental results

We designed a passive fiber for single mode operation with an effective area $\sim 1500\mu\text{m}^2$ at a wavelength of $1.06\mu\text{m}$ in a compact configuration. This was fabricated in a two-step process that enabled us to draw the micro-clad fiber close to the targeted design. First, the hexagonal microstructured cladding elements (canes) were obtained by the stack and draw technique. The canes were then stacked around the central undoped core element in an enclosing silica jacket tube to form a second-stage preform (Fig. 6(a)) wherein each cane was sealed and self-pressurized during the fiber draw. In the cane draw and in stacking of the second stage preform we paid particular attention to limiting twist in the microstructured canes which would otherwise have adversely affected the regularity of the structure. Figure 6(b) shows an electron micrograph of the fabricated fiber. The annotated circle of diameter $2\Lambda_1$ in Fig. 6(b)

passes through the central hole of each microstructured cladding region, showing there was little distortion in the fiber. The dimensions as obtained from the electron micrographs were: $\Lambda_1 = 45 \mu\text{m}$, $d_2/\Lambda_2 = 0.29$, $d_2 = 1.65 \mu\text{m}$ and fiber diameter $240 \mu\text{m}$.

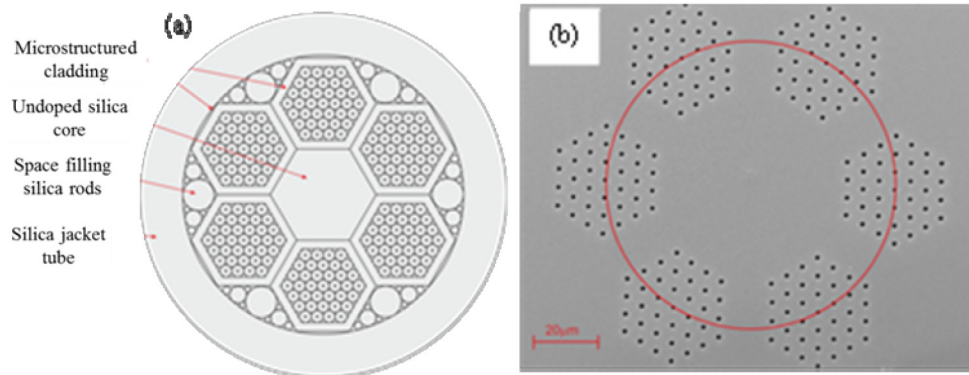


Fig. 6. (a) Schematic of the second stage preform for fabricating the micro-clad LCFs with 6 microstructured cladding elements. Boundaries between elements are shown to illustrate construction of both the first and second stage preforms but these will not be visible in the fiber (b) Electron micrograph of the fabricated micro-clad LCF.

3.1 Fiber characterization

Figure 7 shows the imaged facet of the fiber when light at a wavelength of $1.06 \mu\text{m}$ was coupled to the input end of the fiber and the imaged output illuminated from the side in order to show both the transmitted mode and fiber structure. Without disturbing the setup, images were obtained with and without side illumination.

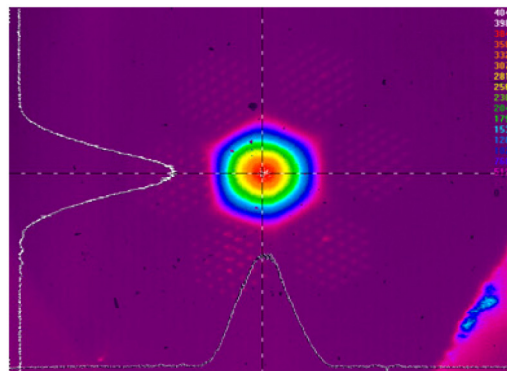


Fig. 7. Fundamental mode image of the fabricated micro-clad LCF at a wavelength of $1.06 \mu\text{m}$.

To estimate the mode field diameter (MFD), widths of the x and y Gaussians at the 13.5% height ($1/e^2$) on the image were measured without side illumination and then scaled using the dimensions of the fiber structure. From this we estimate the effective area to be $\sim 1440 \mu\text{m}^2$. The most interesting aspect of the fabricated fiber was that even when it was loosely bent into a single turn of radius $\sim 40 \text{cm}$, it was robustly single-moded and supported the FM only. A weak two-lobed HOM was observed only when the launch was highly offset from the center. We investigated this further as our simulations had predicted the existence of HOMs for the targeted design. SEM images of the fiber showed that the fiber matched our design reasonably well except that the air holes were somewhat larger ($\sim 1.65 \mu\text{m}$ as compared to $1 \mu\text{m}$ in the designed fiber). Consequently, we simulated the fabricated fiber with dimensions as obtained from the SEM images and our results showed that although the fabricated fiber

supported the higher order LP₁₁ mode, it was well separated from the FM in the effective index space with much higher confinement and bend loss. We did not observe the HOMs in our experiment, which was likely largely due to the fact that the fiber was excited with a Gaussian beam that would have favored the excitation of the fundamental mode.

We then characterized the bend loss of the fabricated fiber. The macrobending loss of the fiber was ~3dB per turn at $R_c = 20\text{cm}$ for all wavelengths $\geq 1.02\mu\text{m}$ up to the optical spectrum analyzer limit of $1.75\mu\text{m}$ (Fig. 8). When bent down to radii smaller than 20cm, the FM was found to be stable with fiber handling away from the imaged end facet. Figure 8 also shows the simulated (macro) bend loss of the fiber, which is in good agreement with the experimentally measured values. The numerical simulations for the modal properties were carried out using COMSOL Multiphysics[®]. An important observation in Fig. 8 is that the low

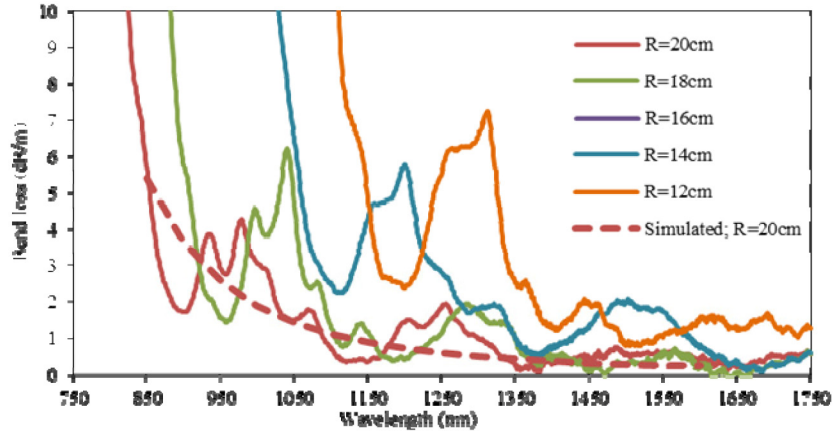


Fig. 8. Experimentally measured bend loss spectrum of the fabricated micro-clad LCF. The red dotted curve is the numerically simulated bend loss of the fiber at a bend radius of 20cm.

wavelength bend loss edge of the fiber shifts towards longer wavelengths as we reduce the bend radius. Thus, besides the FM loss, this behavior would also determine the minimum bend radius limit of the fiber. Finally, we note that during the characterization experiments we observed that the fiber was sensitive to microbending, which we attribute to an insufficiently thick jacket glass in the final fiber. This issue will be addressed in future work.

4. Discussion

4.1 Fiber design for very large fundamental mode area ($> 3000\mu\text{m}^2$)

We simulated micro-clad fibers with larger core diameter (up to $80\mu\text{m}$) based on the proposed concept. Simulations showed that the qualitative behavior of their modes and bend loss remains similar to the trends shown in Fig. 2 and hence proves the potential of this scheme to achieve LMA fibers with very large effective areas. However, maintaining single-mode operation of the larger mode area designs becomes more complex due to the existence of additional HOMs as the core diameter is increased beyond $\sim 50\mu\text{m}$. For example, our simulations showed that the proposed strategy easily allows the design of a fiber that can exhibit an effective area of $\sim 4766\mu\text{m}^2$ at $1.06\mu\text{m}$ along with a FM and LP₁₁ mode loss of 0.1dB/m and 2.7dB/m, respectively (Fig. 9). However, the 2nd HOM of the fiber exhibits a lower loss than that of the FM ($\sim 0.01\text{dB/m}$; Fig. 9(c)). Fortunately, the fractional power of the LP₂₁ mode within the core region is though $< 30\%$, while it is above 77% for the FM (c.f. Figure 9). By employing additional techniques such as a selective launch and strategic mode selective doping, it should be possible to significantly mitigate the issues associated with these detrimental HOMs.

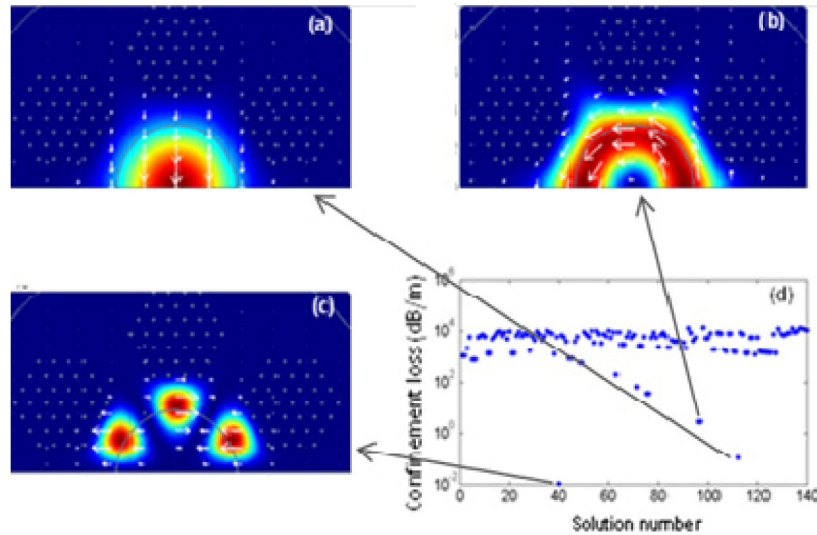


Fig. 9. Optical mode characteristics of the proposed fiber with a core diameter of $80\mu\text{m}$: (a) FM; (b) LP_{11} mode (c) LP_{21} mode; (d) Confinement loss of various modal solutions of the structure. FM effective area $\sim 4766\ \mu\text{m}^2$; FM loss $\sim 0.11\text{dB/m}$; LP_{11} mode loss = 2.7dB/m , fractional power within core: 77% (FM); 53% (LP_{11}); 32% (EH_{21}).

5. Conclusion

In conclusion, we have presented a new design strategy that combines the desirable bending characteristics of all-solid LCFs with the splicing and handling advantages of single-material rod-type PCFs. The design allows for a greater flexibility in controlling the index difference between the core and the cladding through appropriate design of the microstructured cladding elements, which may also be easily individually altered to achieve polarization maintaining characteristics. We fabricated the first micro-clad LCF with FM effective area $\sim 1440\mu\text{m}^2$ at $1.06\mu\text{m}$ and demonstrated its potential to offer compact high power fiber devices. We also showed that better mode discrimination and bending capability as compared to rod-type PCFs for very large effective areas exceeding $3000\mu\text{m}^2$ makes the proposed design highly attractive for achieving extremely large mode area fibers.

Acknowledgments

This work was supported by UK EPSRC through grant EP/H02607X/1 (EPSRC Centre for Advanced Manufacturing in Photonics)